Kinetic effects on a tokamak pedestal ion flow, ion heat transport and bootstrap current

2013 Plasma Phys. Control. Fusion 55 045009

(http://iopscience.iop.org/0741-3335/55/4/045009)

Plasma Phys. Control. Fusion **55** (2013) 045009 (12pp) doi:10.1088/0741-3335/55/4/045009

Kinetic effects on a tokamak pedestal ion flow, ion heat transport and bootstrap current

Peter J Catto[1], Felix I Parra[1], Grigory Kagan[2], Jeffrey B Parker[3], Istvan Pusztai[1,4] and Matt Landreman[1]

[1] Plasma Science and Fusion Center, Massachusetts Institute of Technology, Cambridge, MA 02139, USA
[2] Theoretical Division, Los Alamos National Laboratory, Los Alamos, NM 87545, USA
[3] Princeton Plasma Physics Laboratory, Princeton University, Princeton, NJ 08544, USA
[4] Nuclear Engineering, Applied Physics, Chalmers University of Technology and Euratom-VR Association, SE-41296 Goteborg, Sweden

E-mail: catto@psfc.mit.edu

Received 2 October 2012, in final form 18 February 2013
Published 13 March 2013
Online at stacks.iop.org/PPCF/55/045009

Abstract
We consider the effects of a finite radial electric field on ion orbits in a subsonic pedestal. Using a procedure that makes a clear distinction between a transit average and a flux surface average we are able to solve the kinetic equation to retain the modifications due to finite $\vec{E} \times \vec{B}$ drift orbit departures from flux surfaces. Our approach properly determines the velocity space localized, as well as the nonlocal, portion of the ion distribution function in the banana and plateau regimes in the small aspect ratio limit. The rapid variation of the poloidal ion flow coefficient and the electrostatic potential in the total energy modify previous banana regime evaluations of the ion flow, the bootstrap current, and the radial ion heat flux in a subsonic pedestal. In the plateau regime, the rapid variation of the poloidal flow coefficient alters earlier results for the ion flow and bootstrap current, while leaving the ion heat flux unchanged since the rapid poloidal variation of the total energy was properly retained.

(Some figures may appear in colour only in the online journal)

1. Introduction

Extensions of neoclassical theory to subsonic banana regime pedestals [1–3] with strong density and electric field variation and weaker ion temperature variation [4–6] have recently been called into question [7]. In the following sections we demonstrate that concern is justified, but that the results of [7] must also be corrected. In fact, we find herein corrected banana and plateau regime expressions for the ion particle flow and bootstrap current, and for the ion heat flux in the banana regime. These new large aspect ratio results differ from all those obtained previously [1–3, 7, 8], except for the plateau regime ion heat flux [3, 8]. The disagreements arise because of subtle differences between both the portion of the ion distribution function localized in velocity space to the trapped and barely passing ion region and the nonlocal portion valid for all velocity space. Some of these differences arise because different kinetic equations are solved in [1–3, 8] and [7], and other differences occur because a clear distinction must be made between flux functions and functions of the constants of the motion in both the poloidal flow coefficient and the kinetic and electrostatic potential energy parts of the total energy.

We consider the limit in which the poloidal ion gyroradius $\rho_{pi} = \rho_i B/B_p$ is much larger than the ion gyroradius $\rho_i = v_i/\Omega_i$ by assuming $B/B_p \gg 1$, where B_p is the poloidal magnetic field, $RB_p = |\nabla\psi|$ with ψ the poloidal flux divided by 2π, and $v_i = (2T_i/M)^{1/2}$ the ion thermal speed and $\Omega_i = ZeB/Mc$ the ion gyrofrequency for ions of mass M, charge number Z, and temperature T_i. Unlike standard tokamak kinetic theory, we allow ρ_{pi} to be comparable to the pedestal width for the density, electron temperature, and electric field (without assuming any special scaling for the pedestal width), while requiring it to be small compared with the width of the ion temperature pedestal. For consistency, we allow the poloidal flow coefficient to vary on the same ρ_{pi} scale. This ordering is representative of a high confinement mode pedestal with subsonic flow where the $\vec{E} \times \vec{B}$ drift and the ion diamagnetic drift must cancel to lowest order [4–6]. This behavior has been observed in the helium discharges on DIII-D since the background ion temperature can be measured directly [9], and seems qualitatively consistent with Alcator C-Mod measurements [5, 6].

For a subsonic pedestal the ions must be electrostatically confined to lowest order and the associated radial electric field is then large enough that the $\vec{E} \times \vec{B}$ drift velocity can compete with the poloidal component of the parallel streaming to modify trajectories. These modifications introduce a new dependence on the electric field and its radial variation (the latter is referred to as orbit squeezing [10]) into the neoclassical ion flow via the ion temperature gradient term [11–13]. The constraint that Maxwellian ions are required to make the entropy production vanish requires the ion temperature pedestal to be much wider than ρ_{pi} in a banana or plateau regime pedestal [4, 8]. This slowly varying ion temperature profile assumption is a limitation of the treatment herein, but leads to an analytically tractable model and gives features consistent with experimental observations [5, 6]. Changes in the ion heat flux [1, 3, 7, 8] and the bootstrap current [2, 8] also occur. The precise difference between the $\vec{E} \times \vec{B}$ and ion diamagnetic drifts remains undetermined until conservation of toroidal angular momentum is solved.

All analytic calculations assume large aspect ratio, but numerical calculations that are just becoming available for realistic aspect ratio [14] may ultimately find these analytic results useful to highlight the physics issues at large aspect ratio and low collisionalities where the numerics becomes challenging.

In sections 2 and 3 we briefly review the orbit description employed and the drift kinetic equation solved, before describing our improved localization procedure in section 4. In section 5 we reconsider the banana regime and find that the ion parallel flow, bootstrap current, and the ion heat flux differ from our previous evaluations [1–3] and from [7]. In addition, section 6 reconsiders the plateau regime [3, 8] where we find that the parallel ion flow and bootstrap current change due to orbit squeezing effects, but the radial ion heat flux is not altered. We end with a discussion of our results in section 7.

2. Summary of radial electric field effects on ion orbits

Before presenting our procedure it is convenient to introduce notation and briefly review our treatment of the ion orbits in the presence of electric field effects for $B/B_p \gg 1$ in an axisymmetric tokamak magnetic field $\vec{B} = I\nabla\zeta + \nabla\zeta \times \nabla\psi$, with ζ the toroidal angle.

The large radial electric field $\vec{E} = -\nabla\Phi$ in the pedestal implies that the electrostatic potential $\Phi = \Phi(\psi)$ experienced by an ion varies as the ion drifts radially, where we neglect poloidal angle ϑ and fluctuating corrections to Φ as small. The variation in potential over an orbit width is sufficient to make electrostatic trapping important, even for a flux function potential [1–3]. In addition, the variation of $\partial\Phi/\partial\psi$, referred to as orbit squeezing, enters [10].

It is necessary to carefully retain the distinction between surfaces of constant magnetic flux ψ and drift surfaces of constant canonical angular momentum ψ_*. We consider $B_p/B \ll 1$ so we may employ the drift approximation to the canonical angular momentum

$$\psi_* = \psi - (Iv_\parallel/\Omega_i). \tag{1}$$

The orbit modifications by the strong electric field are evaluated using the total energy

$$E = v^2/2 + (Ze/M)\Phi(\psi), \tag{2}$$

and the magnetic moment $\mu = v_\perp^2/2B$ as velocity space coordinates. Note that we must allow both v^2 and Φ to vary strongly along an ion orbit in (2) even though E is a constant of the motion. It is sometimes convenient to employ the auxiliary pseudokinetic energy variable and constant of the motion

$$E_* \equiv E - (Ze/M)\Phi(\psi_*) = v^2/2 + (Ze/M)[\Phi(\psi) - \Phi(\psi_*)]. \tag{3}$$

We assume the potential only depends quadratically on ψ so that using (1) relates $\Phi(\psi)$ and $\Phi(\psi_*)$ by

$$\Phi(\psi) = \Phi(\psi_*) + (Iv_{||}/\Omega_i)\Phi'(\psi_*) + (1/2)(Iv_\parallel/\Omega_i)^2\Phi'', \tag{4}$$

where Φ'' is a constant, and the prime denotes a derivative with respect to argument.

It is convenient to introduce the effective poloidal $\vec{E} \times \vec{B}$ velocities and the order unity orbit squeezing factor S as

$$u = cI\Phi'/B, \qquad u_* = cI\Phi_*'/B, \qquad \text{and} \qquad S = 1 + cI^2\Phi''/\Omega_i B, \tag{5}$$

with $\Phi'(\psi_*) = \Phi_*'$ and $\Phi'(\psi) = \Phi'$. We may then use $\Phi'(\psi) = \Phi'(\psi_*) + (\psi - \psi_*)\Phi''$ to obtain

$$v_{||} + u = Sv_{||} + u_*. \tag{6}$$

Using the preceding in (3) yields

$$E_* \equiv Sv_\parallel^2/2 + \mu B + u_* v_\parallel = [(Sv_\parallel + u_*)^2/2S] + \mu B - u_*^2/2S = [(v_\parallel + u)^2/2S] + \mu B - u_*^2/2S, \tag{7}$$

that can be solved for $v_\parallel$ to obtain $v_\parallel + u = Sv_\parallel + u_* = \pm(2SE_* + u_*^2 - 2S\mu B)^{1/2}$. When ψ_*, ϑ, E, and μ are used as the coordinates, then one must keep track of $sgn(v_\parallel + u) = sgn(Sv_\parallel + u_*)$ instead of $\mathrm{sgn}(v_\parallel)$. The modified phase space is now split into trapped and passing regions defined by the preceding radicand at the minimum of B, taken as $\vartheta = \pi$. The trapped distribution function must be independent of $sgn(Sv_\parallel + u_*)$ at the bounce points where $(Sv_\parallel + u_*)$ vanishes. The preceding results are valid for arbitrary aspect ratio. Note, however, that at small inverse aspect ratio ε, B will vary by order ε so that for fixed E_* and ψ_* and $u_*^2 \ll v_i^2$, (7) gives $|v_\parallel + (u_*/S)| \sim (\varepsilon/S)^{1/2} v_i$. Consequently, the effective ion–ion collision frequency is $\nu_{\rm eff} \sim \nu_{ii} S/\varepsilon$ and the trapped fraction is $F \sim (\varepsilon/S)^{1/2}$. Moreover, using (1) gives the ion banana width as $\Delta \sim \rho_{\rm pi}(\varepsilon/S)^{1/2}$. Consequently, we expect the ion heat diffusivity in the banana regime to be $F\Delta^2\nu_{\rm eff} \sim (\varepsilon/S)^{1/2}\nu_{\rm ii}\rho_{\rm pi}^2$ for $u \ll v_{\rm i}$. Further details of the trapped fraction estimate are given following equation (15) and the extension of this argument for $u_*^2 \sim v_{\rm i}^2$ is given near the end of section 5.

3. Steady-state drift kinetic equation

Using ψ_*, ϑ, E and μ as our independent variables for an axisymmetric steady-state tokamak results in the drift kinetic equation $\dot{\vartheta}\,\partial f/\partial\vartheta = C\{f\}$ since μ is an adiabatic invariant and $\dot{\psi}_* = 0 = \dot{E}$. Here C denotes the Fokker–Planck collision operator for ion–ion collisions. Working to high enough order to retain $\vec{E}\times\vec{B}$ plus magnetic drifts, $\vec{v}_d$, gives $\dot{\vartheta} = (v_\parallel\vec{n}+\vec{v}_{\rm d})\cdot\nabla\vartheta$ with $\vec{n} = \vec{B}/B$, and results in the steady-state drift kinetic equation

$$(v_\parallel\vec{n}+\vec{v}_{\rm d})\cdot\nabla\vartheta\,\partial f/\partial\vartheta = C\{f\}, \tag{8a}$$

where $\vec{v}_{\rm d} = (v_\parallel/\Omega_{\rm i})\nabla\times(v_\parallel\vec{n})$. This form for the drifts is adequate for our purposes since parallel velocity corrections are unimportant. The conservative form of (8a),

$$\nabla\cdot\{[\vec{B}+(B/v_\parallel)\vec{v}_{\rm d}]f\} = (B/v_\parallel)C\{f\}, \tag{8b}$$

in ψ, ϑ, E and μ variables will be more convenient for forming moments.

To recover a Maxwellian to lowest order we write

$$f = f_*(\psi_*, E) + h(\psi_*, \vartheta, E_*, \mu, t), \tag{9}$$

where

$$f_* = f_*(\psi_*, E)$$
$$= \eta(\psi_*)[M/2\pi T_{\rm i}(\psi_*)]^{3/2}\exp[-ME/T_{\rm i}(\psi_*)], \tag{10}$$

with both the pseudo-density, $\eta(\psi) = n_{\rm i}(\psi)\exp[Ze\Phi(\psi)/T_{\rm i}(\psi)]$, and the ion temperature, $T_{\rm i}(\psi)$, weakly varying functions of space in the pedestal, as required to make the entropy production vanish [5]. Then f_* can be Taylor expanded about ψ even when the ion density $n_{\rm i}$ and the electrostatic potential are allowed to be strong functions of ψ. Expanding (10) about the Maxwellian

$$f_{\rm M} = f_{\rm M}(\psi, E)$$
$$= \eta(\psi)[M/2\pi T_i(\psi)]^{3/2}\exp[-ME/T_i(\psi)], \tag{11}$$

gives

$$f_* = f_{\rm M}\left\{1 - \frac{Iv_\parallel}{\Omega_{\rm i}}\left[\frac{\partial\ell n p_{\rm i}}{\partial\psi} + \frac{Ze}{T_{\rm i}}\frac{\partial\Phi}{\partial\psi} + \left(\frac{Mv^2}{2T_{\rm i}} - \frac{5}{2}\right)\frac{\partial\ell n T_{\rm i}}{\partial\psi}\right] + \cdots\right\}, \tag{12}$$

where $\mathrm{d}\ln p_{\rm i}/\mathrm{d}\ln T_{\rm i} \sim L_T/\rho_{\rm pi} \gg 1$, with L_T the ion temperature scale length. The full correction to $f_{\rm M}$ is $f_* - f_{\rm M} + h$ to the order of interest herein and the kinetic equations (8a) and (8b) becomes

$$(v_\parallel + u)\vec{n}\cdot\nabla\vartheta\,\partial h/\partial\vartheta = C_\ell\{f_* - f_{\rm M} + h\}, \tag{13}$$

where we allow for finite and strongly varying $\boldsymbol{E}\times\boldsymbol{B}$ effects by retaining the u term from $\dot{\vartheta}$, but ignore the magnetic drift correction as small because B is weakly varying (of course, magnetic drift effects are still retained via the distinction between ψ and ψ_*). We use C_ℓ to denote the linearized ion–ion collision operator.

In our previous banana regime work [1–3] we used $C_\ell\{(1, \boldsymbol{v}, v^2/2)f_{\rm M}\} = 0$ to rewrite $C_\ell\{f - f_{\rm M}\} = C_\ell\{h - d_j\}$, with

$$d_1 = f_{\rm M}\frac{I(v_\parallel + u)}{\Omega_{\rm i}}\left(\frac{Mv^2}{2T_{\rm i}} - \frac{5}{2} + a_1\right)\frac{\partial\ell n T_{\rm i}}{\partial\psi}, \tag{14a}$$

for $j = 1$, or equivalently

$$d_2 = f_{\rm M}\frac{I(v_\parallel + u)}{\Omega_{\rm i}}\left(\frac{M(v^2+u^2)}{2T_{\rm i}} - \frac{5}{2} + a_2\right)\frac{\partial\ell n T_{\rm i}}{\partial\psi}, \tag{14b}$$

for $j = 2$. We then attempted to obtain a solution localized to the trapped and barely passing region in the small inverse aspect ratio limit $\varepsilon \ll 1$, where a_1 or a_2 was a flux function to be determined to restore momentum conservation when it became necessary to employ an approximate collision operator to obtain explicit results (note $a_1 \approx a_2 + Mu^2/2T_{\rm i}$ to order ε). The key shortcoming of this procedure is that by assuming the function $h - d$ was localized for $\varepsilon \ll 1$ such that $h - d \propto \sqrt{\varepsilon}$ with a large pitch angle derivative of order $1/\sqrt{\varepsilon}$, we obtained order $\rho_{\rm pi}/L_{\rm T} \ll 1$ corrections to the ion density and temperature that did not vanish in the cylindrical limit as $\varepsilon \to 0$ (as can be seen from the density and energy moments of the d_j).

Shaing and Hsu [7] took issue with our procedure and results and attempted to extend earlier orbit squeezing work. The relevant original work assumed $S \gg 1$, ultimately neglected u^2 corrections as small, and retained only pitch angle scatter [15]. Later work considered finite u when the specified non-flux function electrostatic potential correction due to the 'possible formation' of a shock vanished [16], or considered the subsonic small poloidal Mach number regime that neglects finite u corrections to the ion flow and heat flux, and the bootstrap current [17]. The results of [15–17] contradict our results [1–3] and led to the criticism in [7]. However, it is important to realize that the kinetic equation solved in [7, 15–17] is not valid when finite orbit effects due to a strong pedestal electric field must be retained. This issue is addressed in the appendix to show that if this defect is corrected to account for the strong $\boldsymbol{E}\times\boldsymbol{B}$ effect, the technique of [7] reproduces the results of our previous work [1–3] in the absence of orbit squeezing when the distinction between ψ and ψ_* is ignored in the kinetic energy. Moreover, in [7, 15–17] strong poloidal variation of the drive term proportional to $v^2v_\parallel$ in $f_* - f_{\rm M}$ in (13) due to strong Φ variation on an orbit is neglected (recall (2)) when performing the transit average, and the questionable lowest order approximation $v_\parallel = -u$ is employed on the nonlocal portion of f in [17]. The banana regime results in all these earlier publications differ in their u and S dependences from the new results we present in the next two sections. Physically, some banana regime orbit squeezing cases [7, 15–17] are flawed because they are consistent with a trapped fraction of $(\varepsilon S)^{1/2}$ and an effective collision frequency of $\nu_{ii}/S\varepsilon$ [15], while other cases [1, 3] are incorrect because they are consistent with a trapped fraction estimate of $(\varepsilon S)^{1/2}$.

In the next section we obtain an improved localized solution not having the defect of our earlier treatment. Where appropriate we retain the strong radial variation of the electrostatic potential, the kinetic energy and the poloidal flow coefficient.

4. Localization procedure

Next we focus on obtaining the solution to (13) with the property that as $\varepsilon \to 0$ it will have an explicit nonlocal portion valid for all velocities of order $f_M\rho_{pi}/L_T$, with L_T the ion temperature gradient scale length, and a portion that we must solve for that is localized in velocity space to the trapped-barely passing region such that it only gives $\sqrt{\varepsilon} f_M\rho_{pi}/L_T$ corrections to the density and temperature. The localized portion of f has strong pitch angle variation, and both the local and nonlocal f contributions can have strong radial variation due to orbit squeezing. We introduce the inverse aspect ratio expansion of the magnetic field by taking

$$B_0/B = 1 - 2\varepsilon \sin^2(\vartheta/2) = 1 - \varepsilon + \varepsilon \cos\vartheta, \tag{15}$$

where B_0 is the magnetic field at $\vartheta = 0$. The $\varepsilon = r/R \ll 1$ assumption allows transport to remain local because the trapped and barely passing ion orbit widths are of order $(\varepsilon/S)^{1/2}\rho_{pi}$, and so less than the equilibrium pedestal width that is only allowed to be as small as ρ_{pi}.

We stress that the estimates made at the end of section 3 follow an ion along its trajectory, that is, they hold its canonical angular momentum ψ_* and total energy E (or pseudo-kinetic energy E_*) fixed. We did so using equation (7) to determine the trapped-passing boundary by considering the barely trapped ion trajectory at two points: (i) when the barely trapped banana tip, $(Sv_\| + u_*) = 0$, is at the inboard equatorial plane, and (ii) when the same ion has parallel speed $v_{\|0}$ at the outboard equatorial plane. We then use the B of equation (15) for $\varepsilon \ll 1$ and define $2\mu B_0 = v_{\perp 0}^2$, to obtain

$$[v_{\|0} + (u_{*0}/S_0)]^2 = (2\varepsilon/S_0)[v_{\perp 0}^2 + (2u_{*0}^2/S_0^2)].$$

Based on this expression, the trapped fraction is $(2\varepsilon/S_0)^{1/2}$ and the effective collision frequency is $\nu_{\rm eff} = S_0\nu/2\varepsilon$, for $u_{*0}^2 \ll v_i^2$, as we estimated there. If the estimate is made on a fixed flux surface ψ (instead of for fixed ψ_*) then this flawed procedure leads to the replacement $Sv_{\|0} + u_{*0} \to v_{\|0} + u_0$ on the left side of the preceding equation for $u_0^2 \ll v_i^2$ and results in the incorrect trapped fraction estimate of $(2\varepsilon S_0)^{1/2}$.

With inverse aspect ratio corrections kept through order ε we may write (7) as

$$\begin{aligned}(v_\| + u)^2/2 &= (Sv_\| + u_*)^2/2 = W(1 - \Lambda B/B_0) \\ &= (1-\Lambda)W[1 - \kappa^2 \sin^2(\vartheta/2)],\end{aligned} \tag{16}$$

where W, Λ and κ^2 are ϑ independent constants of the motion through order ε and defined by

$$W = S_0E_* + 2(S_0 - 1)(E_* - \mu B_0) + (3/2)u_{*0}^2 \tag{17}$$

$$\Lambda = \frac{\kappa^2}{\kappa^2 + 2\varepsilon} = \frac{S_0\mu B_0 + 2(S_0-1)(E_* - \mu B_0) + u_{*0}^2}{S_0E_* + 2(S_0-1)(E_*-\mu B_0) + (3/2)u_{*0}^2} \tag{18}$$

$$\kappa^2 = \frac{2\varepsilon\Lambda}{1-\Lambda} = \frac{2\varepsilon[S_0\mu B_0 + 2(S_0-1)(E_*-\mu B_0) + u_{*0}^2]}{S_0(E_* - \mu B_0) + (1/2)u_{*0}^2} \tag{19}$$

with

$$u_{*0} = cI\Phi_*'/B_0, \qquad S_0 = 1 + (cI^2\Phi''/\Omega_0 B_0), \tag{20}$$

and $\Omega_0 = ZeB_0/Mc$. The variables W and Λ reduce to $v^2/2$ and $\lambda = 2\mu B_0/v^2$ when $u_{*0} = 0$ and $S_0 = 1$ where equation (16) reduces to $v_\|^2 = v^2(1 - \lambda B/B_0)$. The trapped-passing boundary is given by $\kappa^2 = 1$ or $\Lambda = 1/(1+2\varepsilon)$, and is shifted and distorted from the usual boundary as noted in [1–3]. Equations (16)–(19) will be convenient for switching between ψ_* and ψ variables so that transit averages that follow an ion trajectory can be performed holding ψ_* fixed, while flux surface averages can be evaluated at fixed ψ.

We desire the nonlocal portion of the ion distribution function f to have the property that it gives the correct parallel ion velocity to lowest order without altering the density and temperature (see (32) and (33)). Consequently, h must be close to the distribution function g defined by

$$g = f_M\frac{Iv_\|}{\Omega_i}\left(\frac{ME}{T_i} - \frac{Ze\Phi(\psi)}{T_i} - \frac{5}{2} + \frac{k(\psi)B^2}{\langle B^2\rangle}\right)\frac{\partial \ell n T_i}{\partial\psi}, \tag{21}$$

where $k = k(\psi)$ is a flux function to lowest order in our $\sqrt{\varepsilon}$ expansion and will be determined ultimately by requiring that our approximate collision operator acting on the localized distribution function conserve momentum (or equivalently, result in no radial ion particle flux). As shown in [14], for finite aspect ratio, k must acquire poloidal variation in the pedestal in order for the continuity equation to be satisfied. However, for the present large aspect ratio case, we may make an ansatz that k is constant on a flux surface to leading order in $\sqrt{\varepsilon}$, and we will verify afterwards that the distribution function we obtain is consistent with this assumption. The B dependence of the k term is made explicit to obtain a form for the flows that will be manifestly divergence free as $\varepsilon \to 0$. Using (21) in (13) along with $C_\ell\{v_\| f_M\} = 0$ yields

$$(v_\| + u)\vec{n}\cdot\nabla\vartheta\,\partial h/\partial\vartheta = C_\ell\{h - g\}; \tag{22}$$

a form for the kinetic equation that is useful in both the banana and plateau regimes.

The function $h - g$ is not properly localized for our purposes because g depends on ψ, ϑ, E and μ rather than ψ_*, ϑ, E and μ, and on $v_\|$ rather than the combination $v_\| + u = Sv_\| + u_*$ that can be used to define the trapped-passing boundary via

$$v_\| + u = Sv_\| + u_* = \pm(2SE_* + u_*^2 - 2S\mu B)^{1/2}, \tag{23}$$

as noted in our discussion of the orbits. As (14*a*) and (14*b*) has been eliminated as flawed, we employ an improved approach that shifts h in a different way. In the banana regime (22) requires $\partial h/\partial\vartheta = 0$ or $h = h(\psi_*, E, \mu)$, where h implicitly depends on the sign of $v_\parallel + u = Sv_\parallel + u_*$ because of (23). Consequently, we may add and subtract a function of the constants of the motion, $Q = Q(\psi_*, E, \mu)$, to h. Moreover, based on (14*a*) and (14*b*) we suspect we want to add to and subtract from (21) a function very close to

$$f_{\mathrm{M}}\frac{Iu}{\Omega_{\mathrm{i}}}\left(\frac{ME}{T_{\mathrm{i}}} - \frac{Ze\Phi(\psi)}{T_{\mathrm{i}}} - \frac{5}{2} + \frac{k(\psi)B^2}{\langle B^2\rangle}\right)\frac{\partial\ell nT_{\mathrm{i}}}{\partial\psi}, \quad (24)$$

but written in terms of the ψ_*, E, μ variables so that h can be shifted. Based on (6) we can see that we should replace u by u_*/S. Moreover, we can continue to treat the spatial variation of I, B, f_{M}, T_{i} and $\partial T_{\mathrm{i}}/\partial\psi$ as slow (the $\partial T_{\mathrm{i}}/\partial\psi$ slow assumption will be discussed in more detail once we obtain explicit results). Consequently, all we need address is the rapid variation of $v^2/2 = E - (Ze/M)\Phi(\psi)$ caused by the possible strong radial electric field and field shear in the pedestal that enter via Φ and k. To deal with the possible rapid variations of Φ and k we introduce the approximate canonical angular momentum variable Ψ_* defined by

$$\Psi_* \approx \psi_* - Iu_*/\Omega_{\mathrm{i}}S = \psi - [I(Sv_\parallel + u_*)/S\Omega_{\mathrm{i}}], \quad (25)$$

where order ε corrections can be safely ignored since we are only interested in the $\sqrt{\varepsilon}$ corrections associated with $Sv_\parallel + u_* = v_\parallel + u \sim v_{\mathrm{i}}(\varepsilon S)^{1/2}$ and its sign (the distinctions between S and S_0 and u and u_0 no longer matter). Using (25) we see that the distance between constant Ψ_* and ψ surfaces is order $\rho_{\mathrm{pi}}(\varepsilon/S)^{1/2}$, which in our ordering is much smaller than the ρ_{pi} distance between constant ψ_* and ψ surfaces.

Based on the preceding discussion we rewrite g as a function of Ψ_*, ϑ, E, μ, and the sign of $Sv_\parallel + u_*$ by introducing a function that only depends on the constants of the motion Ψ_* and E through order $\sqrt{\varepsilon}$, namely

$$Q = f_{\mathrm{M}}\frac{Iu_*}{\Omega_{\mathrm{i}}S}\left(\frac{ME}{T_{\mathrm{i}}} - \frac{Ze\bar{\Phi}_*}{T_{\mathrm{i}}} - \frac{5}{2} + \bar{k}_*\right)\frac{\partial\ell nT_{\mathrm{i}}}{\partial\psi}, \quad (26)$$

where the overbar denotes a dependence on Ψ_* rather than on ψ or ψ_* so that $\bar{\Phi}_* \equiv \Phi(\Psi_*)$ and $\bar{k}_* \equiv k(\Psi_*)$ (the distinction between Ψ_* and ψ is not needed in f_{M}, T_{i}, I and B). Note that we are carefully retaining the distinction between $\bar{\Phi}_* \equiv \Phi(\Psi_*)$ and $\Phi = \Phi(\psi)$, as well as between $\bar{k}_* \equiv k(\Psi_*)$ and $k = k(\psi)$, unlike previous work [1–3, 7, 8, 15–18]. These distinctions matter when we use (25) to Taylor expand Φ and k about Ψ_* to rewrite (21) as

$$g = f_{\mathrm{M}}\frac{I[(Sv_\parallel + u_*) - u_*]}{\Omega_{\mathrm{i}}S}\left(\frac{ME}{T_{\mathrm{i}}} - \frac{Ze[\bar{\Phi}_* + (\psi - \Psi_*)\bar{\Phi}'_*]}{T_{\mathrm{i}}}\right.$$
$$\left. - \frac{5}{2} + [\bar{k}_* + (\psi - \Psi_*)\bar{k}'_*]\right)\frac{\partial\ell nT_{\mathrm{i}}}{\partial\psi}, \quad (27)$$

where $\bar{\Phi}'_* \equiv \Phi'(\Psi_*)$, $\bar{k}'_* \equiv k'(\Psi_*)$ and $Sv_\parallel + u_*$ and u_* are signed quantities. Noting $Sv_\parallel + u_* = v_\parallel + u \sim v_{\mathrm{i}}(\varepsilon S)^{1/2}$ and $u_* \sim v_{\mathrm{i}}$ we retain $\sqrt{\varepsilon}$ corrections by letting

$$H = h + Q \quad (28)$$

and

$$G = g + Q, \quad (29)$$

with

$$G = f_{\mathrm{M}}\frac{I(Sv_\parallel + u_*)}{\Omega_{\mathrm{i}}S}\left(\frac{ME}{T_{\mathrm{i}}} - \frac{Ze\bar{\Phi}_*}{T_{\mathrm{i}}} - \frac{5}{2} + \frac{B^2\bar{k}_*}{\langle B^2\rangle}\right.$$
$$\left. + \frac{Iu_*}{\Omega_{\mathrm{i}}S}\left(\frac{Ze\bar{\Phi}'_*}{T_{\mathrm{i}}} - \frac{B^2\bar{k}'_*}{\langle B^2\rangle}\right)\right)\frac{\partial\ell nT_{\mathrm{i}}}{\partial\psi}, \quad (30)$$

where the drive $G = G(\psi_*, \theta, E, \mu)$ depends on θ, but $H = H(\psi_*, E, \mu)$ is independent of θ to the requisite order as desired. Equation (16) then becomes

$$(v_\parallel + u)\vec{\boldsymbol{n}}\cdot\nabla\vartheta\,\partial H/\partial\vartheta = C_\ell\{H - G\}; \quad (31)$$

with $H - G$ the desired localized portion of the distribution function, where G is the drive term and H is the response with $(H - G)/f_{\mathrm{M}} \sim (\varepsilon/S)^{1/2}(\rho_{\mathrm{pi}}/L_T)$ as desired for the trapped and barely passing.

Using $H \approx G$ equation (28) gives the nonlocal portion of the distribution function to be $f = f_* + g$ since $h \approx G - Q = g$. As a result, ignoring $\sqrt{\varepsilon}$ corrections we obtain the lowest order nonlocal portion of the distribution function as

$$f \approx f_{\mathrm{M}}\left\{1 - \frac{Iv_\parallel}{\Omega_{\mathrm{i}}}\left[\frac{\partial\ell np_{\mathrm{i}}}{\partial\psi} + \frac{Ze}{T_{\mathrm{i}}}\frac{\partial\Phi}{\partial\psi}\right.\right.$$
$$\left.\left. + \left(\frac{Mv^2}{2T_{\mathrm{i}}} - \frac{5}{2}\right)\frac{\partial\ell nT_{\mathrm{i}}}{\partial\psi}\right]\right\} + g + O(\sqrt{\varepsilon}). \quad (32)$$

with g given by (21). Therefore, we find $\int \mathrm{d}^3v f \approx n_{\mathrm{i}}$, $\int \mathrm{d}^3v Mv^2 f \approx 3n_{\mathrm{i}}T_{\mathrm{i}} = 3p_{\mathrm{i}}$, and

$$n_{\mathrm{i}}V_{\parallel\mathrm{i}} = \int \mathrm{d}^3v v_\parallel f$$
$$\approx -\frac{Ip_{\mathrm{i}}}{M\Omega_{\mathrm{i}}}\left[\frac{\partial\ell np_{\mathrm{i}}}{\partial\psi} + \frac{Ze}{T_{\mathrm{i}}}\frac{\partial\Phi}{\partial\psi} - \frac{kB^2}{\langle B^2\rangle}\frac{\partial\ell nT_{\mathrm{i}}}{\partial\psi}\right]$$
$$\approx -\frac{Ip_{\mathrm{i}}}{M\Omega_{\mathrm{i}}}\left[\frac{\partial\ell np_{\mathrm{i}}}{\partial\psi} + \frac{Ze}{T_{\mathrm{i}}}\frac{\partial\Phi}{\partial\psi} - k\frac{\partial\ell nT_{\mathrm{i}}}{\partial\psi}\right], \quad (33)$$

to within $\sqrt{\varepsilon}$ corrections as desired for a proper localization. We remark that using (33) the nonlocal result (32) can be rewritten as $f \approx f_{\mathrm{M}}[1 + (MV_{\parallel\mathrm{i}}v_\parallel/T_{\mathrm{i}}) + O(\sqrt{\varepsilon})]$.

In the following section we apply the preceding to the banana regime.

5. Banana regime

The banana regime calculation is complicated by the need to deal with the collision operator while distinguishing carefully between transit (performed at fixed ψ_*, E, μ) and flux surface (performed at fixed ψ, E, μ) averages. However, the localization of $H - G$ will allow some simplification.

5.1. *Localized portion of ion distribution function*

We begin by noting that in the banana regime $H = H(\psi_*, E, \mu)$ since (31) requires that $(v_\parallel + u)\boldsymbol{n}\cdot\nabla\vartheta\,\partial H/\partial\vartheta = 0$ to lowest order. To next order the poloidal integral over a complete circuit annihilates the left side giving the constraint

$$\oint \frac{\mathrm{d}\vartheta C_\ell\{H-G\}}{(Sv_{||}+u_*)\vec{n}\cdot\nabla\vartheta} = 0, \tag{34}$$

where the integration is to be performed at fixed ψ_* or Ψ_*, E, μ over a full poloidal circuit for the passing ions and over a complete bounce for the trapped ones.

The localization of $H-G$ to the trapped and barely passing region allows the Rosenbluth potential form of the ion–ion collision operator for collisions with a background Maxwellian to be simplified. Unlike the small electric field limit where only pitch angle scattering is kept, the complicated nature of the trapped-passing boundary requires that energy scatter as well as pitch angle scatter must be retained. The flux function k is adjusted to improve the localization by ensuring that the lowest order radial ion particle flux vanishes, or equivalently, that momentum be conserved in ion–ion collisions.

We first give the collision operator in ψ, ϑ, W and Λ variables since the new pitch angle variable Λ is a constant at the trapped-passing boundary and W variation is nearly perpendicular to this boundary. Only scattering normal to the trapped-passing boundary $\Lambda = 1/(1+2\varepsilon)$ (or $\kappa^2 = 1$) is needed because of the localization provided by assuming $\sqrt{\varepsilon} \ll 1$ [19]. Consequently, in the full linearized ion–ion collision operator, Λ derivatives acting on $H-G$ are much larger than W derivatives as long as $\varepsilon \ll 1$ since $H-G \sim G(\varepsilon/S)^{1/2} \sim W\partial(H-G)/\partial W$, but $\partial(H-G)/\partial\Lambda \sim G/(\varepsilon^{1/2}S^{3/2})$ for the trapped and barely passing, while $\partial(H-G)/\partial\Lambda \sim G\varepsilon/S^{3/2}$ for the freely passing. Retaining only collisional scattering normal to the trapped-passing boundary our Rosenbluth collision operator may be approximated by

$$C_\ell\{H-G\} = \frac{1}{j}\frac{\partial}{\partial\Lambda}\left[jf_{\mathrm{M}}\nabla_{\mathrm{v}}\Lambda\cdot\overleftrightarrow{\boldsymbol{D}}\cdot\nabla_{\mathrm{v}}\Lambda\frac{\partial}{\partial\Lambda}\left(\frac{H-G}{f_{\mathrm{M}}}\right)\right], \tag{35}$$

where $\overleftrightarrow{\boldsymbol{D}} = (\nu_\perp/4)(v^2\overleftrightarrow{\boldsymbol{I}} - \vec{v}\vec{v}) + (\nu_\|/2)\vec{v}\vec{v}$, and $j = 1/\nabla_{\mathrm{v}}W\times\nabla_{\mathrm{v}}\Lambda\cdot\nabla_{\mathrm{v}}\varphi \approx BW/SB_0(v_\|+u)$ is the Jacobian, with $\nu_\perp/\nu_{\mathrm{i}} = 3(2\pi)^{1/2}[\mathrm{erf}(x)-\Psi(x)]/(2x^3)$, $\nu_{||}/\nu_{\mathrm{i}} = 3(2\pi)^{1/2}\Psi(x)/(2x^3)$, $x = v/v_{\mathrm{i}}$, $\mathrm{erf}(x)$ the error function, $\Psi(x) = [\mathrm{erf}(x) - x\mathrm{erf}'(x)]/(2x^2)$, ν_{i} is the Braginskii ion–ion collision frequency, and ϕ is the gyrophase with $\nabla_{\mathrm{v}}\varphi = v_\perp^2\vec{n}\times\vec{v}$. Using $\nabla_{\mathrm{v}}\Lambda = -(\Lambda/W)(v_\|+u)\vec{n} + (1-\Lambda B/B_0)[S_0\vec{v}_\perp + 2(S_0-1)v_\|\vec{n}+\cdots] \approx -(\Lambda/W)(v_\|+u)\vec{n}$ from [3] gives the required operator, namely

$$C_\ell\{H-G\} = \frac{(v_\|+u)}{B}\frac{\partial}{\partial\Lambda} \times\left[B\Lambda W^{-2}(v_\|+u)\vec{n}\cdot\overleftrightarrow{\boldsymbol{D}}\cdot\vec{n}f_{\mathrm{M}}\frac{\partial}{\partial\Lambda}\left(\frac{H-G}{f_{\mathrm{M}}}\right)\right]. \tag{36}$$

Equation (36) is easily written in terms of the Ψ_*, θ, W and Λ variables so that the transit averages can be performed using (6), (7) and (16)–(18):

$$C_\ell\{H-G\} = \frac{(Sv_\|+u_*)}{B}\frac{\partial}{\partial\Lambda} \times\left[B\Lambda W^{-2}(Sv_\|+u_*)\vec{n}\cdot\overleftrightarrow{\boldsymbol{D}}\cdot\vec{n}f_{\mathrm{M}}\frac{\partial}{\partial\Lambda}\left(\frac{H-G}{f_{\mathrm{M}}}\right)\right], \tag{37}$$

where $\rho_{\mathrm{pi}}/L_{\mathrm{T}} \sim B_{\mathrm{p}}/B \ll \varepsilon^{1/2}$ is assumed to neglect corrections from $\partial\Psi_*/\partial\Lambda$. We neglect order ε corrections to pre-factors, so we may use $\Lambda \approx 1$ for the trapped and barely passing as found from (7) and (18) with $Sv_\| + u_* = v_\| + u \approx 0$.

We need to only evaluate the coefficient $\vec{n}\cdot\overleftrightarrow{\boldsymbol{D}}\cdot\vec{n}$ for the trapped and barely passing. We may now employ $v_\| \approx -u \approx -u_*/S$ to complete the specification of the collision operator in both sets of variables since $H-G$ is localized to the trapped-barely passing region. We note that $W \approx S_0\mu B_0 + u_{*0}^2/S_0 \approx S_0\mu B_0 + S_0u^2$ and $v^2 \approx 2W/S - u^2 \approx 2W/S_0 - u_{*0}^2/S_0^2$ since in the coefficient of the localized term we can neglect $\sqrt{\varepsilon}$ order corrections. Using these results allows us to write $\vec{n}\cdot\overleftrightarrow{\boldsymbol{D}}\cdot\vec{n}$ in both sets of variables:

$$\vec{n}\cdot\overleftrightarrow{\boldsymbol{D}}\cdot\vec{n} \approx W\nu_\perp/2S + (\nu_\| - \nu_\perp)u^2/2 \approx W\nu_\perp/2S_0 + (\nu_\| - \nu_\perp)u_{*0}^2/2S_0^2, \tag{38}$$

where the collision frequencies depend on v^2 but it no longer varies significantly since $\Psi_* - \psi \sim RB_{\mathrm{p}}\rho_{\mathrm{pi}}(\varepsilon/S)^{1/2} \ll RB_{\mathrm{p}}\rho_{\mathrm{pi}}$.

As usual, $H = 0$ for the trapped particles since the transit average is over a full bounce with $\oint \mathrm{d}\vartheta C_\ell\{G\}/[(Sv_\|+u_*)\vec{n}\cdot\nabla\vartheta] = 0$ and H cannot depend on $sgn(Sv_\| + u_*)$. The transit averages can be performed in essentially the usual manner [10–12, 18] since from (16) $(Sv_\|+u_*)\partial(Sv_\|+u_*)/\partial\Lambda = -WB/B_0$. For the passing $\partial H/\partial\Lambda$ must be determined from (34), (37) and (38) in the Ψ_*, θ, W and Λ variables. Ignoring ε corrections, recalling that $\vec{n}\cdot\overleftrightarrow{\boldsymbol{D}}\cdot\vec{n}$ and f_{M} do not depend on $\Lambda \approx 1$ to lowest order, and integrating (34) with (37) inserted from $\Lambda = 0$, then within the limitations of our collision model we find the passing response

$$\frac{\partial H}{\partial\Lambda} = \frac{\oint \mathrm{d}\vartheta(Sv_\|+u_*)\partial G/\partial\Lambda}{\oint \mathrm{d}\vartheta(Sv_\|+u_*)} \approx -\frac{(f_{\mathrm{M}}IW/\Omega_{\mathrm{i}}S)}{\langle v_\|+u\rangle}\left[\frac{Mv^2}{2T_{\mathrm{i}}} - \frac{5}{2} + k + \frac{Iu}{\Omega_{\mathrm{i}}}\left(\frac{Ze\Phi'}{T_{\mathrm{i}}} - k'\right)\right] \times\frac{\partial\ell nT_{\mathrm{i}}}{\partial\psi}, \tag{39a}$$

so that

$$\frac{\partial(H-G)}{\partial\Lambda} \approx -\left(\frac{1}{\langle v_\|+u\rangle} - \frac{1}{v_\|+u}\right)\left(\frac{f_{\mathrm{M}}IW}{\Omega_{\mathrm{i}}S}\right) \times\left[\frac{Mv^2}{2T_{\mathrm{i}}} - \frac{5}{2} + k + \frac{Iu}{\Omega_{\mathrm{i}}}\left(\frac{Ze\Phi'}{T_{\mathrm{i}}} - k'\right)\right]\frac{\partial\ell nT_{\mathrm{i}}}{\partial\psi}, \tag{39b}$$

where we use $\bar{\Phi}_* \equiv \Phi(\Psi_*) \approx \Phi(\psi) = \Phi$, $\bar{k}_* \equiv k(\Psi_*) \approx k(\psi) = k$, $\bar{\Phi}'_* \approx \Phi'$, $\bar{k}'_* \approx k'$, and $Sv_\| + u_* = v_\| + u$; replace the transit average by a flux surface average $\langle\ldots\rangle$; and use $u \approx u_*/S$ since only the trapped and barely passing contribute. Note the desired localization in pitch angle in (39b) as $\partial(H-G)/\partial\Lambda \sim \varepsilon^{-1/2}S^{-3/2}(\rho_{\mathrm{pi}}/L_T)f_{\mathrm{M}}$ since $Sv_\| + u_* = v_\| + u \sim (\varepsilon S)^{1/2}v_{\mathrm{i}}$.

5.2. Determining the flow coefficient k

Before using (40) to evaluate k we verify that its ϑ dependence is unimportant as it is order $\sqrt{\varepsilon}$. Forming the continuity equation from (8a) and (8b), using

$\nabla \cdot \{[\vec{B} + (B/v_\parallel)\vec{v}_\mathrm{d}]f_*\} = 0$ and number conservation $\int \mathrm{d}^3 v C = 0$, recalling $h = g + (h - g)$, and noting that g is odd in $v_\parallel$, leaves $\nabla \cdot \{\int \mathrm{d}^3 v[hv_\parallel \vec{n} + (h - g)\vec{v}_\mathrm{d}]\} = 0$. To lowest order in the $\sqrt{\varepsilon}$ expansion $h = g$, giving $\nabla \cdot (\int \mathrm{d}^3 v h v_\parallel \vec{n}) \sim (n_\mathrm{i} v_\mathrm{i}/qR)(\rho_\mathrm{pi}/L_T)[\partial k/\partial\vartheta + O(\varepsilon^{1/2})]$. The remaining term depends on the localized portion of the distribution function that varies radially on the ρ_pi scale, and gives an order ε smaller contribution of $\nabla \cdot [\int \mathrm{d}^3 v(h - g)\vec{v}_\mathrm{d}] \sim (n_\mathrm{i} v_\mathrm{i} \rho_\mathrm{i}/\rho_\mathrm{pi} R)(\varepsilon^{1/2}\rho_\mathrm{pi}/L_T)$. Consequently, we estimate $\partial k/\partial\vartheta \sim \varepsilon^{1/2}$.

We choose $\bar{k}_* \approx k$ by demanding our localized response $H - G$ conserve momentum and thereby ensure ambipolarity. To see that these are equivalent to the order we require, we form the flux surface averaged $(v_\parallel/B)(Iv_\parallel/\Omega_\mathrm{i})$ moment of the conservative form of the drift kinetic equation to find the equation to find $\langle \int \mathrm{d}^3 v f \vec{v}_\mathrm{d} \cdot \nabla\psi \rangle = \langle \nabla \cdot [(I/\Omega_\mathrm{i}) \int \mathrm{d}^3 v f v_\parallel \vec{v}_\mathrm{d}] \rangle$, where we use $\int \mathrm{d}^3 v v_\parallel C = 0$ and $\vec{v}_\mathrm{d} \cdot \nabla(Iv_\parallel/B) = 0$ from equation (25) of [20]. The flux surface average radial ion particle flux $\langle \int \mathrm{d}^3 v f \vec{v}_\mathrm{d} \cdot \nabla\psi \rangle$ must be small (by a square root of the mass ratio) to equal the flux surface average radial electron particle flux in order to maintain ambipolarity. As a result, it must be that $\langle \nabla \cdot [(I/\Omega_\mathrm{i}) \int \mathrm{d}^3 v f v_\parallel \vec{v}_\mathrm{d}] \rangle$ is also very small, and we may use either $\int \mathrm{d}^3 v v_\parallel C = 0$ or $\langle \int \mathrm{d}^3 v f \vec{v}_\mathrm{d} \cdot \nabla\psi \rangle = 0$ to determine k to ensure both momentum conservation and intrinsic ambipolarity.

We determine flow coefficient k from $\int \mathrm{d}^3 v v_\parallel C = \int \mathrm{d}^3 v(v_\parallel + u)C_\ell\{H - G\} = 0$ by integrating by parts and using

$$\int_0^{B_0/B} \mathrm{d}\Lambda \left(\frac{1}{\sqrt{1 - \Lambda B/B_0}} - \frac{1}{\langle \sqrt{1 - \Lambda B/B_0} \rangle} \right) \approx 1.38\sqrt{2\varepsilon}, \tag{40}$$

where this result is insensitive to the lower limit as long as it is much less than $\sqrt{\varepsilon}$. Using (40) to perform the integrals in $\int \mathrm{d}^3 v(v_\parallel + u)C_\ell\{H - G\} = 0$, the differential equation for k is determined as a ratio of W integrals to be

$$\frac{Iu}{\Omega_\mathrm{i}} \left(\frac{\partial k}{\partial\psi} - \frac{Ze}{T_\mathrm{i}} \frac{\partial\Phi}{\partial\psi} \right) - k + \frac{5}{2} + U^2 = \sigma(U^2), \tag{41}$$

where

$$\sigma \equiv \frac{\int_o^\infty \mathrm{d}y \mathrm{e}^{-y}(y + 2U^2)^{3/2}[y\nu_\perp(x) + 2U^2\nu_\parallel(x)]}{\int_o^\infty \mathrm{d}y \mathrm{e}^{-y}(y + 2U^2)^{1/2}[y\nu_\perp(x) + 2U^2\nu_\parallel(x)]}, \tag{42}$$

with $U^2 = Mu^2/2T_\mathrm{i}$, $y = MW/T_\mathrm{i}S - 2U^2 = x^2 - U^2 = Mv^2/2T_\mathrm{i} - U^2$, and $B \approx B_0$ in U and u. Note that for $U^2 \to \infty$, $\sigma \to 2U^2$, while for $U^2 \to 0$, $\sigma \to 1.33$.

The preceding agrees with the conventional result for $u = 0$; however, it differs from all previous evaluations because of the k' and Φ' terms on the left in (41) with the k' term due to the rapid radial variation of the poloidal flow coefficient and the Φ' due to the rapid radial variation of the kinetic energy $v^2/2 = E - Ze\Phi/M$ in the $v_\parallel v^2$ term in (12). Using $(ZeIu/\Omega_\mathrm{i} T_\mathrm{i})(\partial\Phi/\partial\psi) = 2U^2$ equation (41) can be rewritten as

$$k - \frac{Iu}{\Omega_\mathrm{i}} \frac{\partial k}{\partial\psi} = \frac{5}{2} - U^2 - \sigma(U^2). \tag{43}$$

A strict quadratic relation between Φ and ψ leads to a linear relation or one-to-one mapping between U and ψ that allows us to assume $k = k(U)$. Then we may use $(Iu/\Omega_\mathrm{i})(\partial k/\partial\psi) = 2U^2(S - 1)(\partial k/\partial U^2)$ in (43) to obtain

$$k - 2U^2(S - 1)\frac{\partial k}{\partial U^2} = \frac{5}{2} - U^2 - \sigma(U^2), \tag{44}$$

(recall $B \approx B_0$ in S). Interestingly, these changes for $S = 1$ give $k = (5/2) - U^2 - \sigma(U^2)$, making the poloidal flow reverse sign sooner than in our previous results [1–3, 19] since the sign of U^2 has changed because of the new term $(ZeIu/\Omega_\mathrm{i} T_\mathrm{i})(\partial\Phi/\partial\psi) = 2U^2$ retained in (30). This observation seems to be in better agreement with what is seen in a recent simulation [14] at larger ε and ν_i. However, the strict quadratic assumption that leads to the single valued mapping between U and ψ and $(Iu/\Omega_\mathrm{i})(\partial k/\partial\psi) = 2U^2(S - 1)(\partial k/\partial U^2)$ makes the rapid radial variation of the coefficient k depend on S in an unphysical way as we now demonstrate.

To find k more generally for constant S we use the dummy variable $z = U^2$ and let $q = 1/[2(S - 1)]$, then (43) becomes

$$\frac{\partial}{\partial z}\left(\frac{k}{z^q}\right) = -q\frac{(5/2) - z - \sigma(z)}{z^{q+1}}, \tag{45}$$

that has the obvious homogeneous solution of z^q. Integrating from $z = 0$ to U^2 for $S < 1$ and from $z = U^2$ to ∞ for $1 < S < 3/2$, and then letting $\eta = z/U^2$, gives

$S < 1$ (or $q < 0$):

$$k = -q\int_0^1 \mathrm{d}\eta \frac{(5/2) - U^2\eta - \sigma(U^2\eta)}{\eta^{1+q}} \to \begin{cases} 1.17 & U^2 = 0 \\ -3U^2/(3 - 2S) & U^2 \to \infty \end{cases}$$

and

$1 < S < 3/2$ (or $q > 1$):

$$k = q\int_1^\infty \mathrm{d}\eta \frac{(5/2) - U^2\eta - \sigma(U^2\eta)}{\eta^{1+q}} \to \begin{cases} 1.17 & U^2 = 0 \\ -3U^2/(3 - 2S) & U^2 \to \infty. \end{cases} \tag{46}$$

To extend the range of q to include $0 < q < 1$ we introduce $\sigma(0) \approx 1.33$ into the form between (45) and (46) and rewrite it to obtain

$S < 1$ (or $q < 0$) and $S > 3/2$ (or $0 < q < 1$):

$$k = \frac{5}{2} - \sigma(0) + q\int_0^1 \mathrm{d}\eta \frac{U^2\eta + \sigma(U^2\eta) - \sigma(0)}{\eta^{1+q}} \to \begin{cases} 1.17 & U^2 = 0 \\ 3U^2/(2S - 3) & U^2 \to \infty. \end{cases} \tag{47}$$

We are not interested in the region near $q = 0$ (for which $k = \text{constant}$) since $S \to \pm\infty$, which is outside the regime of validity of our expansions that assume $S \sim 1$.

Plots of k versus U^2 for various S are given in figure 1 and illustrate the dramatic change in behavior of the flow coefficient in (33) that occurs about $S = 3/2$. Note that a change in the sign of k typically occurs for $U^2 < 1$ if $1/2 < S < 3/2$,

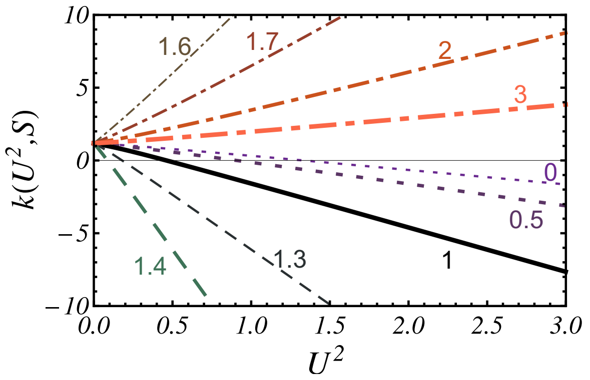

Figure 1. Plots of k versus U^2 for various S in the banana regime illustrating the dramatic change in behavior about $S = 3/2$. A change in the sign of k typically occurs for $U^2 < 1$ if $1/2 < S < 3/2$, while for $S > 3/2$ the sign of is always positive.

while for $S > 3/2$ the sign of is always positive. A question remains as to the behavior of k for $q \approx 1$ (or $S \approx 3/2$). In this limit, if we also consider small z, we find the solution $k = [(5/2) - \sigma(z = 0)] + [1 + \sigma'(z = 0)]qz/(1 - q) + \beta z^q$, with β undetermined since z^q is a homogeneous solution. Letting $\beta = -[1 + \sigma'(z = 0)]/(1 - q)$ gives a solution well behaved at $q = 1$ for $z \ll 1$ to be $k = [(5/2) - \sigma(z = 0)] + [1 + \sigma'(z = 0)](qz - z^q)/(1 - q) + \cdots$, since for $q \to 1$ this becomes $k \to [(5/2) - \sigma(z = 0)] + [1 + \sigma'(z = 0)]z(\ln z - 1) + \cdots$. Also, at large z, where $\sigma \to 2z$, there is a similar solution $k = 3qz/(1 - q) + \beta z^q$, but a *different* choice of β, $\beta = -3/(1 - q)$, is required to remove the $q = 1$ singularity (and obtain the logarithmic solution $k = 3z(\ln z - 1) + \cdots$). Consequently, the different choice for β means that a solution k for all z is not possible when $S = 3/2$ (or $q = 1$).

The behavior of k versus U^2 in the vicinity of $S = 3/2$ is unphysical. It is a consequence of a strict quadratic potential profile assumption and our assumption of a locally linear ion temperature profile. Consequently, to find k, it is better to employ (43) rather than (44).

5.3. Evaluation of the ion heat flux and bootstrap current

Next, we evaluate the radial ion heat flux using the lowest order $Iv^2(v_\parallel/B)^2$ moment of the conservative form of the drift kinetic equation to obtain

$$\langle \vec{q} \cdot \nabla\psi \rangle = -\frac{McIT_{\rm i}}{Ze}\left\langle \int \frac{d^3v}{B}\left(\frac{Mv^2}{2T_{\rm i}} - \frac{5}{2}\right) v_\parallel C_\ell\{H - G\} \right\rangle, \tag{48}$$

where because of momentum, energy and number conservation the pre-factor replacement $v_\parallel(v^2 - 5T_{\rm i}/M) \to (v_\parallel + u)(v^2 + u^2)$ may be employed, and then an integration by parts. Inserting (39*a*) and (39*b*) and (41), using j, and noting that the localized nature of $H - G$ allows the approximation $M(v^2 + u^2)/2T_{\rm i} \approx MW/T_{\rm i}S$ to be used, gives

$$\langle \vec{q} \cdot \nabla\psi \rangle = \frac{\pi MI^2}{S^3\Omega_{\rm i}^2 T_{\rm i}}\frac{\partial T_i}{\partial\psi}\int dW\, d\Lambda f_M W^2\left(\frac{MW}{T_{\rm i}S} - \sigma\right) \times[\nu_\perp v^2 + (2\nu_\parallel - \nu_\perp)u^2]\left(\frac{1}{\langle v_\parallel + u\rangle} - \left\langle\frac{1}{v_\parallel + u}\right\rangle\right), \tag{49}$$

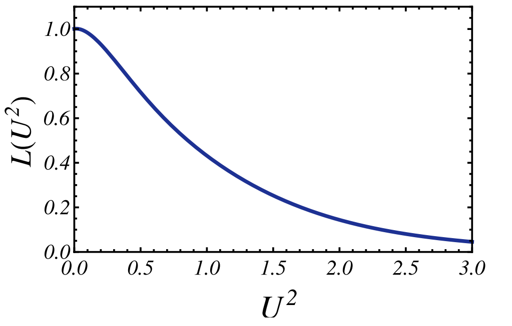

Figure 2. The monotonic fall-off of L with increasing U^2 is shown for the function entering the coefficient of the banana regime ion heat flux.

where one $1/S$ comes from j, another from $\partial(H - G)/\partial\Lambda$, and the third from $M(v^2 + u^2)/2T_{\rm i} \approx MW/T_{\rm i}S$. Using (16) and (40) the preceding becomes

$$\langle \vec{q} \cdot \nabla\psi \rangle = -1.38\sqrt{\varepsilon}\frac{\pi MI^2}{S^3\Omega_{\rm i}^2 T_{\rm i}}\frac{\partial T_i}{\partial\psi} \times \int dW f_M W^{3/2}\left(\frac{MW}{T_{\rm i}S} - \sigma\right)[\nu_\perp v^2 + (2\nu_\parallel - \nu_\perp)u^2],$$

where to the requisite order $x^2 = Mv^2/2T_{\rm i} = MW/T_{\rm i}S - U^2$. Introducing $y = MW/T_{\rm i}S - 2U^2 = x^2 - U^2$ this becomes

$$\langle \vec{q} \cdot \nabla\psi \rangle = -1.38\sqrt{\frac{\varepsilon}{S}}\frac{p_{\rm i}I^2\exp(-U^2)}{\sqrt{2\pi}M\Omega_{\rm i}^2} \times\frac{\partial T_{\rm i}}{\partial\psi}\int_0^\infty dy(y + 2U^2)^{3/2}(y + 2U^2 - \sigma) \times[\nu_\perp y + 2\nu_\parallel U^2]\exp(-y) \tag{50}$$

or

$$\langle \vec{q} \cdot \nabla\psi \rangle = -1.35\sqrt{\frac{\varepsilon}{S}}\frac{p_{\rm i}I^2\nu_{\rm i}L(U^2)}{M\Omega_{\rm i}^2}\frac{\partial T_{\rm i}}{\partial\psi}, \tag{51}$$

with

$$L = 1.53\exp(-U^2)\int_0^\infty dy(y + 2U^2)^{3/2} \times(y + 2U^2 - \sigma)(y + U^2)^{-3/2}\{y[\mathrm{erf}(x) - \Psi(x)] + 2U^2\Psi(x)\}\exp(-y) \tag{52}$$

and $L(0) = 1$. Equations (51) and (52) correct our previous result for the ion heat flux given by (69) of [1] and (1) of errata [3], and also corrects the results of [7, 15–18]. In figure 2 we plot the monotonic fall-off of L with increasing U^2.

The ion heat flux result of (51) can be qualitatively estimated as follows. At fixed ψ_* and $S > 1$, the step size Δ is reduced by orbit squeezing of the banana width giving $\Delta \sim \rho_{\rm p}(\varepsilon/S)^{1/2}$, the effective collision frequency $\nu_{\rm eff}$ is increased by orbit squeezing to $\nu_{\rm eff} \sim \nu_{\rm ii}S/\varepsilon$, and the trapped fraction F is $F \sim (\varepsilon/S)^{1/2}\exp(-U^2)$ since it is decreased by orbit squeezing and exponentially reduced by moving the trapped population out onto the tail of the Maxwellian. We can then estimate the ion heat diffusivity $\chi \sim F\Delta^2\nu_{\rm eff} \sim (\varepsilon/S)^{1/2}\nu_{\rm ii}\rho_{\rm p}^2\exp(-U^2)$, where the detailed U^2 dependence is sensitive to the details of the trapped-passing boundary because this introduces energy scatter. Heat transport due to the passing ions is expected to be of order $\varepsilon\nu_{ii}\rho_p^2$ so all evaluations implicitly assume $\exp(-U^2) \gg \varepsilon^{1/2}$.

Note that since the model assumes constant S, the ion heat flux $\langle\vec{q}\cdot\nabla\psi\rangle$is unable to stay constant across the pedestal when only n_i and U^2 vary in the local result of (51) and both result in a monotonically decreasing behavior. It seems likely that the model needs to retain more physics since we would like to allow $S = 1$ at the top of the pedestal with $S > 1$ in the pedestal (and even changing sign), and $\partial T_i/\partial\psi$ varying across the pedestal in such a manner that $\partial T_i/\partial\psi$ becomes more negative to make up for the monotonic drop off of the n_i and U^2 dependence as well as any variation in S. Without the added features of variation in $\partial T_i/\partial\psi$ and $\partial^2\Phi/\partial\psi^2$ we are forced to assume that the constant ion temperature gradient is maintained in a banana regime pedestal by some anomalous process, modeled as a heat sink in [14], or by energy exchange with the electrons or neutrals, or possibly a subtle orbit loss mechanism that acts as a sink for heat but not particles.

To complete the results we give the corrected expression for the bootstrap current that depends on k because of the friction of the electrons with the ions:

$$J_{\|}^{\rm bs} = -1.46\varepsilon^{1/2}\frac{cIB}{\langle B^2\rangle}\left[\frac{Z^2+2.21Z+0.75}{Z(Z+1.414)}\right] \times\left[\frac{{\rm d}p}{{\rm d}\psi} - \frac{(2.07Z+0.88)n_e}{(Z^2+2.21Z+0.75)}\frac{{\rm d}T_e}{{\rm d}\psi} -k(U^2,S)\frac{n_e}{Z}\frac{{\rm d}T_i}{{\rm d}\psi}\right], \tag{53}$$

where $p = p_i + p_e$, $p_e = n_eT_e$, $n_e = Zn_i$, and we have simply modified the coefficient of the ion flow contribution in [13]. Note when k becomes negative the bootstrap current is enhanced.

Normally a trace impurity flow is measured rather than the flow of the background ions. The poloidal flow of Pfirsch–Schluter trace impurities and banana or plateau regime background ions is given by

$$V_{\rm pol}^z \approx -\frac{cIB_pT_i}{Ze\langle B^2\rangle}\left[\frac{\partial\ell n p_i}{\partial\psi} - \frac{ZT_z}{Z_zT_i}\frac{\partial\ell n p_z}{\partial\psi} -k(U^2,S)\frac{\partial\ell n T_i}{\partial\psi}\right], \tag{54}$$

where the subscript and superscript z is used to denote the impurity quantities. Note the sensitivity to k remains.

6. Plateau regime

It is reasonably straightforward to perform the plateau regime calculation once the collision operator is operating on the localized function $h - g$ since then $C_\ell\{h-g\}$ may then be replaced by $-\nu(h-g)$ on the right side of (22). In the plateau regime the trapped particles are collisional and the singular behavior associated with the streaming operator acting on h at $v_\| + u = 0 = Sv_\| + u_*$ is resolved and independent of the collision operator or even the collision frequency ν that we take as a constant. Consequently, in the plateau regime we need to only solve

$$(Sv_\| + u_*)\vec{n}\cdot\nabla\vartheta\,\partial h/\partial\vartheta = -\nu(h-g), \tag{55}$$

with the ϑ derivative performed holding E, μ and ψ_* fixed. The localized plateau regime solution is $h - g$. Consequently, we must solve the usual plateau form for the kinetic equation

$$(Sv_\| + u_*)\vec{n}\cdot\nabla\vartheta\,\partial(h-g)/\partial\vartheta + \nu(h-g) = -(Sv_\| + u_*)\vec{n}\cdot\nabla\vartheta\,\partial g/\partial\vartheta. \tag{56}$$

In $\partial g/\partial\theta$ we use the results from [8]

$$(Sv_\| + u_*)\vec{n}\cdot\nabla\vartheta\,\partial(v^2/2)/\partial\vartheta = [u_* + (S-1)v_\|](\mu B + v_\|^2)\vec{n}\cdot\nabla\ell n B, \tag{57}$$

$$(Sv_\| + u_*)\vec{n}\cdot\nabla\vartheta\,\partial(v_{||}/\Omega_i)/\partial\vartheta = -(1/\Omega_i)(v_\|^2 + \mu B)\vec{n}\cdot\nabla\ell n B, \tag{58}$$

and

$$(Sv_\| + u_*)\vec{n}\cdot\nabla\vartheta\,\partial(v_{||}B)/\partial\vartheta = -[\mu B - (2S-1)v_{||}^2 - 2u_*v_{||}]\vec{B}\cdot\nabla\ell n B. \tag{59}$$

In contrast to previous work [8] we keep the contribution from $\partial k/\partial\vartheta$ evaluated at fixed ψ_* that arises from the ψ dependence of k, namely

$$(Sv_\| + u_*)(\vec{n}\cdot\nabla\vartheta)\partial k(\psi)/\partial\vartheta \approx I(\partial k/\partial\psi)(Sv_\| + u_*) \times(\vec{n}\cdot\nabla\vartheta)\partial(v_\|/\Omega_i)/\partial\vartheta. \tag{60}$$

Then we may rewrite (56) as

$$(Sv_\| + u_*)\partial(h-g)/\partial\vartheta + \nu qR(h-g) = v_iK\sin\vartheta. \tag{61}$$

with

$$K = \frac{\varepsilon If_M}{v_i\Omega_i}\frac{\partial\ell n T_i}{\partial\psi}\left\{(v_\|^2+\mu B) \times\left[\frac{2(\mu B - u_*v_\|) + (3-2S)v_\|^2}{v_i^2} - \frac{5}{2} + \frac{Iv_\|}{\Omega_i}\frac{\partial k}{\partial\psi}\right] +k[\mu B - (2S-1)v_{||}^2 - 2u_*v_{||}]\right\}. \tag{62}$$

Solving for $(h - g)$ as in [8] gives the localized solution

$$h - g \approx \pi v_iK\delta(Sv_{||} + u_*)\sin\vartheta = \pi v_iK\delta(v_{||} + u)\sin\vartheta, \tag{63}$$

in which we may use $v_\| = -u$ in K.

Now that we have the corrected solution for $(h - g)$ we may determine the differential equation for the flow coefficient k in (33) by demanding that there is no lowest order ion particle flux, $0 = \int {\rm d}^3v f\vec{v}_d\cdot\nabla\psi = -(\varepsilon I/2qR\Omega_i)\int {\rm d}^3v(v_\perp^2 + 2v_\|^2)(h-g)\sin\vartheta$, as in [8]:

$$k - \frac{Iu}{\Omega_i}\frac{\partial k}{\partial\psi} = -\frac{1}{2}J(U^2), \tag{64}$$

with

$$J = J(U^2) = \frac{1 + 4U^2 + 6U^4 + 12U^6}{1 + 2U^2 + 2U^4}, \tag{65}$$

in agreement with our earlier results for $\partial k/\partial\psi = 0$ [3, 8]. Note that for $U = 0$, $k = -1/2$ as required, and as $U^2 \to \infty$, $J \to 6U^2$ giving the same limiting form for (64) as in the banana regime case of (43).

For a single valued mapping between U^2 and ψ, using $(Iu/\Omega_i)(\partial k/\partial\psi) = 2U^2(S-1)(\partial k/\partial U^2)$ again leads to unphysical results near $S = 3/2$ as can be seen by introducing

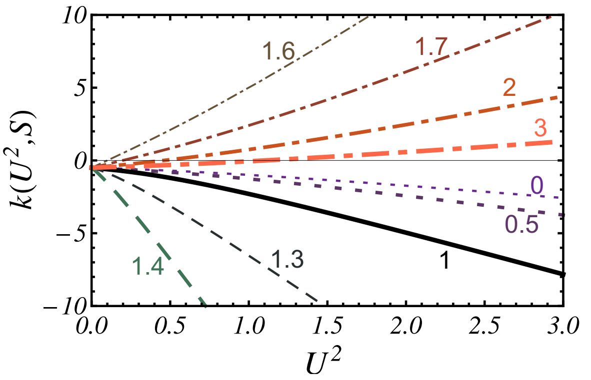

Figure 3. Plots of k versus U^2 for various S in the plateau regime are presented. The behavior is similar to the banana regime, but the sign of k is always negative for $0 < S < 3/2$.

$\eta = z/U^2$ and $q = 1/[2(S-1)]$ to obtain the following forms:

$S < 1$ or $S > 3/2$ (or $q < 1$)

$$k = -\frac{1}{2} + \frac{q}{2}\int_0^1 \mathrm{d}\eta \frac{[J(U^2\eta) - 1]}{\eta^{1+q}} \rightarrow \begin{cases} -1/2 & U^2 = 0 \\ 3U^2/(2S-3) & U^2 \rightarrow \infty, \end{cases} \tag{66}$$

$1 < S < 3/2$ (or $q > 1$)

$$k = -\frac{1}{2} - \frac{q}{2}\int_1^\infty \mathrm{d}\eta \frac{[J(U^2\eta) - 1]}{\eta^{1+q}} \rightarrow \begin{cases} -1/2 & U^2 = 0 \\ -3U^2/(3-2S) & U^2 \rightarrow \infty. \end{cases} \tag{67}$$

Once again $S = 3/2$ (or $q = 1$) presents a problem because of a singularity. In this case, if we consider $q \approx 1$ and $z \ll 1$, we find the solution $k = -1/2 + qz/(1-q) + \beta z^q + \cdots$, with z^q the homogeneous solution. Letting $\beta = -1/(1-q)$ gives a well-behaved solution at $q = 1$ for $z \ll 1$ to be $k = -1/2 + (qz - z^q)/(1-q) + \cdots$, which for $q \rightarrow 1$ becomes $k \rightarrow -1/2 + z(\ln z - 1) + \cdots$. Also, at large z, where $J \rightarrow 6z - 3 + \cdots$, there is a similar solution $k = 3qz/(1-q) + \beta z^q$, the same as in the banana regime. Again the different choice of β, $\beta = -3/(1-q)$, required to remove the $q = 1$ singularity means that a solution for k for all z is not possible when $S = 3/2$.

In figure 3 we plot the flow coefficient k in (33) versus U^2 for various S in the plateau regime. The behavior is similar to that in the banana regime, again showing unphysical behavior about $S = 3/2$. This behavior is again due to the linear T_i and quadratic Φ profile assumptions. The sign of k remains negative in the plateau regime for $0 < S < 3/2$.

In the plateau regime case, the flux surface average radial ion flux $\langle\int \mathrm{d}^3v f \vec{v}_\mathrm{d} \cdot \nabla\psi\rangle$ again must be small to balance the flux surface average radial electron flux to maintain ambipolarity so momentum conservation and ambipolarity are again equivalent constraints to determine k. Moreover, in the plateau regime the localized part of the distribution function is order ε, and, as a result, the poloidally varying piece of the poloidal flow in the plateau regime is smaller than in the banana regime, $\partial k/\partial\vartheta \sim \varepsilon$.

The poloidal flow of Pfirsch–Schluter trace impurities and plateau regime background ions is given by (54).

For completeness we form the ion heat flux, $\langle\vec{q}_\mathrm{i} \cdot \nabla\psi\rangle = \langle\int \mathrm{d}^3v(Mv^2/2) f \vec{v}_\mathrm{d} \cdot \nabla\psi\rangle$, and observe that the result is the same as in [8], namely

$$\begin{aligned}\langle\vec{q}_\mathrm{i} \cdot \nabla\psi\rangle &= -\langle(\varepsilon I M/4qR\Omega_\mathrm{i}) \\ &\quad\times \int \mathrm{d}^3v v^2(v_\perp^2 + 2v_\parallel^2)(h-g)\sin\vartheta\rangle \\ &= -3\sqrt{\frac{\pi}{2}}\frac{I^2\varepsilon^2 n_\mathrm{i}}{qR\Omega_\mathrm{i}^2}\left(\frac{T_\mathrm{i}}{M}\right)^{3/2}\frac{\partial T_\mathrm{i}}{\partial\psi}P(U^2),\end{aligned} \tag{68}$$

where

$$P = P(U^2) = \mathrm{e}^{-U^2}\frac{1 + 4U^2 + 8U^4 + [4(4U^6 + U^8)/3]}{1 + 2U^2 + 2U^4}. \tag{69}$$

Note that the heat flux across a plateau pedestal can be kept constant by assuming $U^2 \ll 1$ at the top of the pedestal and having the peak of P at $U^2 \sim 0.8$ located at the separatrix, but the density drop allowed is only about a factor of two. The ion heat flux is reduced exponentially as the collisionally resolved singularity moves to the tail of the Maxwellian, but it is independent of S since the collisional smearing width $\xi = (v_\parallel + u)/v \sim (qR\nu_\mathrm{ii}/v_\mathrm{i})^{1/3} \ll 1$ is larger than the trapped fraction width $(\varepsilon/S)^{1/2}$. The collisional smearing width is obtained [12] by balancing streaming and velocity space diffusion: $\xi v/qR \sim \nu_\mathrm{ii}\partial^2/\partial\xi^2$. Using $\Delta \sim \rho v_\mathrm{i}/R\nu_\mathrm{eff}$, $\nu_\mathrm{eff} \sim \nu_\mathrm{ii}/(qR\nu_\mathrm{ii}/v_\mathrm{i})^{2/3}$ and $F \sim (qR\nu_\mathrm{ii}/v_\mathrm{i})^{1/3}\exp(-U^2)$ gives the plateau estimate $\chi \sim F\Delta^2\nu_\mathrm{eff} \sim (q\rho^2 v_\mathrm{i}/R)\exp(-U^2)$.

In the bootstrap current expression in [8], $J/2$ must be replaced by $-k$, where they are related by (64) and coincide for $S = 1$. Therefore,

$$\begin{aligned}J_\parallel^\mathrm{bs} &= -\frac{\sqrt{\pi}(\sqrt{2} + 4Z)}{2Z(Z + \sqrt{2})}\frac{\varepsilon^2 c v_\mathrm{e}}{q\nu_\mathrm{ee}} \\ &\quad\times\left[\frac{\mathrm{d}p}{\mathrm{d}\psi} + \frac{(\sqrt{2} + 13Z)n_\mathrm{e}}{2(\sqrt{2} + 4Z)}\frac{\mathrm{d}T_\mathrm{e}}{\mathrm{d}\psi} - k(U^2, S)\frac{n_\mathrm{e}}{Z}\frac{\mathrm{d}T_\mathrm{i}}{\mathrm{d}\psi}\right],\end{aligned} \tag{70}$$

with $v_\mathrm{e} = (2T_\mathrm{e}/m)^{1/2}$, $\nu_\mathrm{ee} = 4(2\pi)^{1/2}n_\mathrm{e}e^4\ln\Lambda/(3m^{1/2}T_\mathrm{e}^{3/2})$, and m the electron mass.

7. Discussion

We have presented an improved evaluation of the ion orbits and a generalized kinetic treatment that allows us to properly determine the localized portion of the ion distribution function in the banana and plateau regimes in the small aspect ratio limit by accounting for the rapid variation of the poloidal ion flow coefficient as well as the electrostatic potential. We retain finite drift departures from flux surfaces by a procedure allowing a clear distinction between transit averages and flux surface averages. The resulting expressions for the ion flow and heat flux, and bootstrap current correct all previous results in the banana regime for a subsonic pedestal [1–3, 5–7, 15–18]. Our plateau regime results also correct earlier expressions for the ion flow and bootstrap current in the presence of orbit squeezing and verify the correctness of the ion heat flux result

[3, 6, 13]. In the banana regime the corrections to prior work are due to the radial variation of both the electrostatic potential in the total energy and the poloidal flow coefficient, while in the plateau regime the changes are associated with poloidal flow coefficient only (so the previous $S = 1$ results are correct). In addition, the results in [7, 15–17] are incorrect for the reasons just stated, and also because the kinetic equation solved is not consistent with (13) as explained in the appendix. Finally, we would be remiss if we did not comment further on the unusual sensitivity of the ion poloidal flow and bootstrap current to orbit squeezing S. As S is increased beyond 3/2, the bootstrap current abruptly decreases because of the abrupt change in the poloidal ion flow direction. This unphysical behavior is a consequence of restricting our analysis to a locally linear ion temperature profile and a quadratic potential profile. The ion heat flow does not display this same sensitivity; however, our result does not allow constant heat flux across the pedestal so an ion heat sink is required. Work is now underway to remove these limitations.

Acknowledgments

Work supported by the US Department of Energy grants at DE-FG02-91ER-54109 at MIT and DE-AC52-06NA-25396 at LANL, and the European Communities under Association Contract between EURATOM and Vetenskapsradet. During the preparation of this paper some of the authors enjoyed the hospitality and support of the Wolfgang Pauli Institute in Vienna, Austria (PJC, FIP, ML), Asociación EURATOM-CIEMAT Laboratorio Nacional de Fusión in Madrid, Spain (PJC, FIP, ML, JBP), and Leverhulme Trust at Oxford University in England (PJC, FIP).

Appendix

We demonstrate that the difference between our former ion poloidal flow, ion heat flux, and bootstrap current expressions [1–3] and those of Shaing and Hsu [7] for $S = 1$ is entirely due to their failure to account for certain $\vec{E} \times \vec{B}$ modifications in the drive term of their drift kinetic equation (24). We first write their distribution function (22) in terms of our f_* and f_M as

$$f = f_M + \left[\frac{M}{T}V_{||} + \frac{2Mq_{||}}{5Tp}\left(\frac{Mv^2}{2T} - \frac{5}{2}\right)\right]v_{||}f_M + \widehat{g}$$
$$= f_*(\psi_*, E) + \frac{Mf_M}{T}\left[V^\vartheta + \frac{2q^\vartheta}{5p}\left(\frac{Mv^2}{2T} - \frac{5}{2}\right)\right]Bv_{||} + \widehat{g}, \tag{A1}$$

where we suppress species subscripts, account for their use of a drifting Maxwellian, and let $\widehat{g}$ denote the remaining portion of the distribution function supposedly given by their (24). In (A1) according to their (56), (57), (60), and (64) and our first form of (33) we have

$$V^\vartheta = \frac{V_{||}}{B} + \frac{cIT}{ZeB^2}\left(\frac{p'}{p} + \frac{Ze\Phi'}{T}\right) = -\frac{\mu_2 2q^\vartheta}{\mu_1 5p} = \frac{kcIT'}{Ze\langle B^2\rangle}, \tag{A2}$$

and

$$q^\vartheta = \frac{q_{||}}{B} + \frac{5cIpT'}{2ZeB^2} = \frac{5cIpT'}{2Ze\langle B^2\rangle}. \tag{A3}$$

The distinctions between B^2 and $\langle B^2\rangle$ in (A2) and (A3) are important to keep the particle and heat flows divergence free. Not surprisingly, the μ_j coefficents are where a key difference between our results and those of [7] arises since $k = -\mu_2/\mu_1$. To see whether this is the difficulty we consider the situation in the absence of orbit squeezing effects by taking $S = 1$ and $u_* = u$.

Forming the kinetic equation for f of (A1) using (8*a*) (recalling that the gradients are performed at fixed E and μ) and using $\nabla \cdot \{[\vec{B} + (B/v_{||})\vec{v}_d]f_*\} = 0$ gives

$$(v_{||}\vec{n} + \vec{v}_d) \cdot \nabla\, \widehat{g} - C_\ell\{\widehat{g}\} = \frac{Mv^2 f_M}{2T}\left(\frac{1}{2} - \frac{3v_{||}^2}{2v^2} - \frac{2uv_{||}}{v^2}\right)$$
$$\times\left\{\left[V^\vartheta + \frac{2q^\vartheta}{5p}\left(\frac{Mv^2}{2T} - \frac{5}{2}\right)\right]\right\}\vec{n}\cdot\nabla B, \tag{A4}$$

where f_M, T, T', V^ϑ, q^ϑ/p and v^2 are assumed to be slowly varying in the radial direction, and we use (7) to obtain the $S = 1$ version of (59), namely

$$(v_{||}\vec{n} + \vec{v}_d)\cdot\nabla(Bv_{||}) = (v_{||} + u)\vec{n}\cdot\nabla(Bv_{||})$$
$$= (v_{||} + u)\vec{n}\cdot\nabla[B(v_{||} + u)]$$
$$= -\tfrac{1}{2}(v^2 - 3v_{||}^2 - 4uv_{||})\vec{n}\cdot\nabla B. \tag{A5}$$

In deriving (A5) it is convenient to replace ψ by ψ_* in B and in other slow functions of ψ and use $(v_{||}\vec{n} + \vec{v}_d)\cdot\nabla\psi_* = 0$. We have ignored the rapid variation of $v^2 = E - Ze\Phi/M$ as in [1–3, 7], but it should be retained as explained in section 4 since there is a contribution from

$$(Ze/M)(v_{||}\vec{n} + \vec{v}_d)\cdot\nabla\Phi = (Ze\Phi'/M)\vec{v}_d\cdot\nabla\psi$$
$$= uv_{||}\vec{n}\cdot\nabla(v_{||}/B) = -(u/2B)(v^2 + v_{||}^2)\vec{n}\cdot\nabla B. \tag{A6}$$

As in [7], we must assume V^ϑ is a flux function through order ε, when in fact the poloidal variation of V^ϑ is formally $\varepsilon^{1/2}$ as discussed preceding (22), and therefore it should also be included. We also neglect the inertial correction $V_\parallel$ in (A4) as small, just as in [7] after (24).

Equation (A4) differs from (24) in Shaing and Hsu [7]. Due to the u terms in (A5) our result contains $(v^2 - 3v_{||}^2 - 4uv_{||})$ instead of $(v^2 - 3v_{||}^2)$ in the overall coefficient. This correction ultimately appears in the μ_j coefficients evaluated at $v_\parallel \approx -u$. As a result, the replacement

$$\left(\frac{1}{2} - \frac{3v_{||}^2}{2v^2}\right) \approx \left(\frac{1}{2} - \frac{3u^2}{2v^2}\right) \to \left(\frac{1}{2} - \frac{3v_{||}^2}{2v^2} - \frac{2uv_{||}}{v^2}\right)$$
$$\approx \left(\frac{1}{2} + \frac{u^2}{2v^2}\right). \tag{A7}$$

must be made in the μ_j coefficients of their (29) to obtain the proper coefficients

$$\mu_j = 1.38(2\varepsilon/\pi)^{1/2}\int_{U^2}^{\infty} dy\,\nu_D F y^{3/2}$$
$$\times\left(y - \frac{5}{2}\right)^{j-1}\left(1 + \frac{U^2}{y}\right)^{1/2}\exp(-y), \tag{A8}$$

where F is defined in (48) of [7]. When the corrected form of μ_j as given by (A7) is employed in place of their (47), then the Shaing and Hsu [7] banana regime expressions for V^ϑ, $\langle \vec{q}_i \cdot \nabla\psi \rangle$ and $J_{||}^{bs}$ agree with those of [1–3]. However, as pointed out in section 4 and noted here, equation (24) of [7] and the results of [1–3] mistakenly assume v^2 to be a constant. In addition, when orbit squeezing is retained the strong radial dependence of V^ϑ via $k = -\mu_2/\mu_1$ that is ignored in this appendix and in [1–3, 5–7, 15–18] must be retained.

Consequently, this appendix demonstrates that the technique of [7] gives the same results as [1] when the proper kinetic equation is employed. We remark that in the standard core calculation the approximation $u = 0$ is employed so the replacement of (A7) no longer matters and either kinetic equation can be used.

References

[1] Kagan G and Catto P J 2010 *Plasma Phys. Control. Fusion* **52** 055004
Kagan G and Catto P J 2010 *Plasma Phys. Control. Fusion* **52** 079801

[2] Kagan G and Catto P J 2010 *Phys. Rev. Lett.* **105** 045002

[3] Catto P J, Kagan G, Landreman M and Pusztai I 2011 *Plasma Phys. Control. Fusion* **53** 054004
Catto P J, Kagan G, Landreman M and Pusztai I 2011 *Plasma Phys. Control. Fusion* **53** 089501

[4] Kagan G and Catto P J 2008 *Plasma Phys. Control. Fusion* **50** 085010

[5] Marr K D, Lipschultz B, Catto P J, McDermott R M, Reinke M L and Simakov A N 2010 *Plasma Phys. Control. Fusion* **52** 055010

[6] Kagan G, Marr K D, Catto P J, Landreman M, Lipshultz B and McDermott R 2011 *Plasma Phys. Control. Fusion* **53** 025008

[7] Shaing K C and Hsu C T 2012 *Phys. Plasmas* **19** 022502

[8] Pusztai I and Catto P J 2010 *Plasma Phys. Control. Fusion* **52** 075016
Pusztai I and Catto P J 2010 *Plasma Phys. Control. Fusion* **52** 119801

[9] DeGrassie J 2008 private communication, General Atomics

[10] Hazeltine R D 1989 *Phys. Fluids* **B 1** 2031

[11] Hinton F L and Hazeltine R D 1976 *Rev. Mod. Phys.* **48** 239

[12] Hirshman S P and Sigmar D J 1981 *Nucl. Fusion* **21** 1079

[13] Helander P and Sigmar D J 2002 *Collisional Transport in Magnetized Plasmas* (*Cambridge Monographs on Plasma Physics*) ed M G Haines *et al* (Cambridge: Cambridge University Press)

[14] Landreman M and Ernst D 2012 *Plasma Phys. Control. Fusion* **54** 115006

[15] Shaing K C and Hazeltine R D 1992 *Phys. Fluids* B **4** 2547

[16] Shaing K C, Hsu C T and Dominguez N 1994 *Phys. Plasmas* **1** 1168

[17] Shaing K C, Hsu C T and Hazeltine R D 1994 *Phys. Plasmas* **1** 3365

[18] Landreman M and Catto P J 2011 *Plasma Phys. Control. Fusion* **53** 015004

[19] Rosenbluth M N, Hazeltine R D and Hinton F L 1972 *Phys. Fluids* **15** 116

[20] Parra F I and Catto P J 2010 *Phys. Plasmas* **17** 056106